

Compatibilization of polycarbonate/poly (ethylene terephthalate) blends by addition their trans-esterification product

Majid Habibelahi, Morteza Ehsani*, Jalil Morshedian

Department of polymer processing, Iran polymer and petrochemical Institute, Tehran, 14977-13115, Iran

*M.Ehsani@ippi.ac.ir; Tel:+98 21 48662502; Fax: +98 21 44787021-3

DOI: 10.22063/poj.2018.2271.1121

Received: 2 August 2018, Accepted: 2 September 2018

ABSTRACT

In this study, poly carbonate (PC) and poly (ethylene terephthalate) (PET) are reactive melt blended with two different conditions to produce copolymers made of them. For each condition, samples are taken at specified mixing times representative a specific structure of copolymers and each one employed to physically compatibilize a PC/PET blend with fixed composition. Reactive blending and copolymer structure are described by solubility analysis results. Continues declining and going through a dip are two trends of solubility versus mixing time depending on reactive blending condition. Decreasing and increasing patterns of solubility curves were attributed to the formation of longer and shorter block length copolymers respectively and the level of solubility is related to the amount of produced copolymers. Differential scanning calorimetry (DSC) and scanning electron microscopy (SEM) techniques were employed to investigate blend compatibility. The content and structure of copolymers showed favorable correlation of T_g differences of blend components and PET crystallinity. As expected, T_g of blend components approached each other by addition of copolymers and longer block length copolymers caused less T_g differences. PET melting point and crystallinity are affected by introducing the copolymers too. Melting endotherms of compatibilized blends comprise a shoulder in addition of the main melting endotherm which the corresponding melting point and crystallinity are related to copolymer structure in which higher melting points and crystallinity are achieved by longer block length copolymers or its higher amounts. SEM micrographs show better dispersion of PET particles in PC matrix including smaller and more uniform particles after copolymer addition. There is a strong correlation between blend morphology and the achieved level of blend compatibility. The more compatibilized PC/PET blend the better dispersion of PET particles in PC matrix is formed. This study could be a basis for design. and production of compatibilizers suitable to achieve a desired level of compatibility in PC and polyester blends specially PC/PET one.

Keywords: PET; PC; trans-esterification; compatibility; crystallinity.

INTRODUCTION

Blending methods attract significant attentions for preparing new materials because of its convenience and affordability than synthesizing the new material. Due to this aim, different blends with various types have been prepared for diverse applications like automotive industry [1], electrical industry[2], packaging [3] and biomedical applications[4]. PET has been introduced as a proper candidate for packaging industry thanks to appropriate mechanical properties, proper chemical resistance and high transparency [5, 6]. However, some drawbacks like low heat deflection temperature and impact strength hampered its usage [7]. PC as an engineering polymer has excellent transparency and toughness whereas it suffers from weak chemical resistance. Blending has been utilized for compensating the PC flaws to achieve the high performance PC based blend [8]. PC/PET blend can be an excellent material while blend immiscibility is a hindrance for such blend which miscibility can be improved by assisting nano materials and modifiers [9]. Moreover, blending method can be ameliorate the miscibility, for instance, reactive blending of PC and PET has been utilized for this aim. In this method, a catalyst triggers and progresses trans-esterification reaction in which copolymers composed of PC and PET were produced [10]. This subject has undergone extensive studies usually aimed to find parameters in relation to an effective reaction. Different types of freshly added catalysts [11] or PET contained catalysts [12], catalyst content [13], blend composition [14], mixing time [15] and mixing temperature [16] could be taken into account. Researchers have studied this reaction in the solid state of PC and PET blends[17] too. The rheology [18], spectroscopic [19], microscopic [20], thermal [11] and solubility [21] techniques have been employed to evaluate the reaction and microstructure of the corresponding copolymers.

The in situ blend compatibilization through the copolymers has been used for this purpose. In such compatibilization method, the reactions are not fully controlled and as a result unavoidable side reactions occur through which degradation of blend components could adversely affect the blend properties. To overcome these drawbacks, the copolymer could be prepared separately and by addition into the blends, compatibility is achieved [22].

Oxazoline in reaction with polypropylene is used by Jeziorska [23] as a compatibilizer for PC/PET blends. He reports that the compatibilized PC/PET blends has one T_g in between those of the neat components. Moreover, PET crystallinity and melting temperature were raised by compatibilization. The solubility analysis and measurement of the intrinsic viscosity indicated that the produced PC and PET block copolymers successfully compatibilized the blend[23].

Ma et al. [24] produced PC and PET random copolymers by trans-esterification reaction and the achieved copolymers were added into PC/PET blends to compatibilize them in the melt state.

Glass transition temperature of PC/PET blends with various amounts of a compatibilizer was studied. Results revealed that, T_g difference of the components decreased with higher content of copolymer which at 60 wt% concentration only one T_g was observed indicating the blend miscibility.

Xue et al. [25] employed a bifunctional epoxy to compatibilize PC and poly(trimethylene terephthalate) (PTT) blends. T_g of the polyester in the compatibilized PC/PTT blend was higher than that of the un-compatibilized blend. Moreover, crystallization of epoxy compatibilized PC/PTT blends was studied [26]. PTT crystallization behavior was disrupted by PC addition resulting in lower melting temperature and crystallinity content.

In this work, PC and PET copolymers were produced by reactive blending in the presence of a freshly added catalyst. After that, copolymers were added to a defined composition of PC/PET blend. The achieved compatibility resulted from copolymer addition was evaluated by DSC and SEM techniques and it was related to the content and microstructure of copolymers. The findings were correlated to solubility analysis, a traditional method to qualitatively evaluate the copolymer microstructure in PC and PET reactive blending.

EXPERIMENTAL

Materials and methods

PC (grade 712) with MFI of 9.5 g (10 min)⁻¹ (at 250°C and 10 kg force, measured by Gottferd MFI instrument model MI-4 made by Germany and located in Research and Technology of Iranian National Petrochemical Company) was obtained from Khuzestan Petrochemical Company of Iran. PC (grade SC1100) with MFI of 9.0 g (10 min)⁻¹ (at 250°C and 10 kg, reported by the producer) was prepared from Samsung Company of South Korea, and PET (grade 821) with intrinsic viscosity of 0.82 dLg⁻¹ (reported by the producer) was obtained from Tondgooyan Petrochemical Company of Iran. The catalyst, lanthanum acetylacetonate was purchased from Merck of Germany, triggered the trans-esterification reaction. Triphenyl phosphate was purchased from Merck of Germany as an inhibitor of trans-esterification reaction.

At first, PC 712 and PET were dried at 100 °C for 24 h. The blends were prepared in a 50 millilitre Brabender internal mixer. PC and PET with 80:20 wt% composition was melt blended for 15 min in the absence of freshly added catalyst. After that, known as premixing, acetylacetonate lanthanum catalyst was added into the mixture and mixing was continued for 20 min according to Table 1.

Table 1. PC and PET Reactive blending conditions.

Sample code	T (°C)	Premixing time (min)	Rotor speed (rpm)	Catalyst content (wt %)
C1	280	15	50	0.20
C2	270	15	30	0.15

The criterion to choose condition is formation of different and specified copolymer structures with varied block lengths. The lower temperature and catalyst content in C2 condition are set to produce relatively long block length copolymers. On the other hand, higher temperature and amount of catalyst in C1 condition formed not only long block length copolymers but also the shorter block length copolymer at longer reaction times.

Table 2 represents sampling times during reactive blending of PC and PET to prepare the copolymers.

Table 2. Sampling times during PC and PET reactive melt blending under C1 & C2 mixing conditions.

Condition Code	Mixing time (min)			
	5	10	15	20
C1	C1R5		C1R15	C1R20
C2	-	C2R10	-	C2R20

The sample codes in Table 2 comprising the mixing condition (C1 or C2) followed by sampling time (the number after R). For example, C1R5 is attributed to the sample was prepared with C1 condition and taken at 5th min of the mixing. PC 1100, PET and the products of C1 or C2 series were dry blended and then melt mixed for 5 min at 270°C in constant composition of 66.5/28.5/5 wt%. In the beginning of the mixing, 1 wt% of triphenyl phosphate was added to the blend to prevent reaction happening during mixing.

For solubility analysis, 1 g of PC/PET blend was dissolved in 50 mL of dichloromethane within 24 h under stirring at room temperature, then filtrated and weighed after drying at 80°C. The solubility was calculated through dividing mass of soluble fraction by initial mass of blend (1 gr).

For thermal analysis, a Perkin Elmer equipment (DSC882e model, USA) from Research and Technology of Iranian National Petrochemical Company was used. The analysis was conducted on soluble and precipitated fractions. The temperature increased in the range of 25 to 280°C with the rate of 10°C/min and under nitrogen atmosphere to avoid thermal degradation.

SEM images (Vega XMU made by Tescan Company of Czech Republic) was utilized for morphology evaluation. Sheets of 2 mm thickness were prepared by hot press at 260°C and cryogenically fractured under liquid nitrogen. The fractured cross-sections were etched by

trifluoroacetic acid for 4 h to remove PET phase and then rinsed in water. The etched surfaces were dried overnight in an oven at 80°C and were coated by a thin layer of gold.

RESULTS AND DISCUSSION

Solubility

To prepare structurally different copolymers, PC and PET were melt blended under C1 and C2 condition (table 1). Fig. 1 shows the curves of solubility versus mixing time, as a measure of trans-esterification progress.

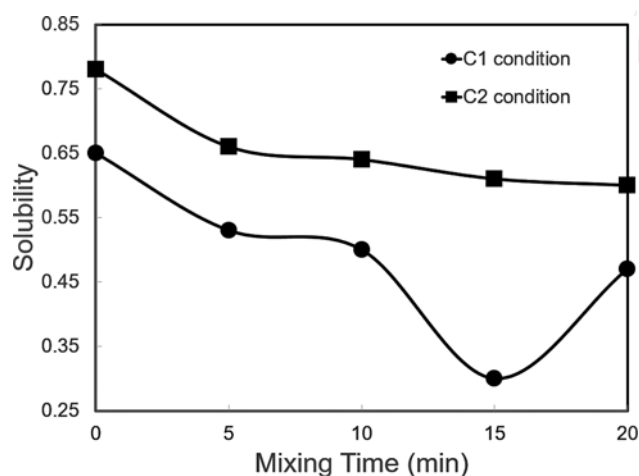


Figure 1. Solubility versus mixing time for C1 and C2 processing condition with dichloromethane as the solvent.

With C1 condition, a dip centered after 15 min of mixing was developed. Mixing under C2 condition resulted in reduction of solubility over the entire mixing time.

The solubility reduction was attributed to the formation of PC and PET block copolymers which were not soluble in dichloromethane. The pattern of solubility with mixing time under C2 condition indicated that the production of PC and PET copolymers continued to the end of mixing time. In comparison to C2 condition, the lower level of solubility which reduced with a steeper slope was achieved by C1 condition. These differences represented the higher rate and more extensive reaction in the second condition. The reduction was followed by higher solubility after 15 min of the mixing because of dissolving the earlier produced copolymers in dichloromethane. Copolymers participating in the reaction under C1 condition made the block length shorter and this new chemical structure helped the copolymers to become soluble in dichloromethane. Considering C1 condition, sampling was conducted in 5, 15 and 20 min of the mixing. These

durations corresponded to the earlier stage of reaction, the maximum amount of produced long block length copolymers and formation of short block length copolymers, respectively. The simpler solubility pattern with C2 condition limited the sampling times to 10 and 20 min of the mixing corresponding to the middle and end of mixing times respectively.

Thermal properties

Figure 2 and Tables 3 and 4 show Tg of the blends through DSC analysis.

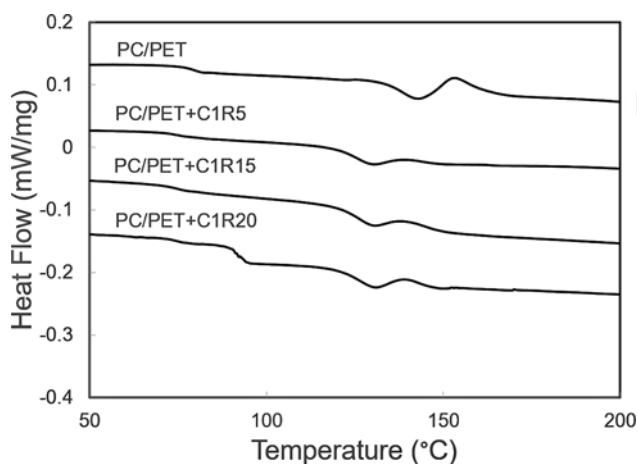


Figure 2. Tg of PC and PET components for blends with and without C1 series products.

Table 3. Thermal properties of PC/PET blend components after compatibilization by C1 series products.

Sample code	T _g PET (°C)	T _g PC (°C)	ΔT _g (°C)	T _{m1} (°C)	T _{m2} (°C)	ΔH1 (J/g)	ΔH2 (J/g)	ΔH2/ΔH (%)
Neat PC/PET	78	138	60	234	-	8.12	-	0
PC/PET+C1R5	80	125	45	231	240	5.51	3.88	41
PC/PET+C1R15	82	119	37	232	243	4.48	5.19	54
PC/PET+C1R20	75	122	47	232	242	3.92	4.28	52

Table 4. Thermal properties of PC/PET blend components after compatibilization by C2 series products.

Sample code	T _g PET (°C)	T _g PC (°C)	ΔT _g (°C)	T _{m1} (°C)	T _{m2} (°C)	ΔH1 (J/g)	ΔH2 (J/g)	ΔH2/ΔH (%)
Pure PC/PET	78	138	60	234	-	8.12	-	0
PC/PET+C2R10	71	122	50	236	244	5.79	5.56	49
PC/PET+C2R20	70	123	53	235	244	6.32	5.93	48

Figure 2 reveals that the neat PC/PET blend exhibits two T_gs at 78 and 138 °C related to PET and

PC respectively which indicates blend immiscibility. Mixing this immiscible blend with C1R5 increased Tg of PET to 80.1°C and reduced that of PC to 125°C. The difference in Tg of blend components, hereafter named as Tg difference (ΔT_g), decreased from nearly 60°C for neat blend to 45°C after C1R5 addition. C1R15 had the same but greater effect on Tg of blend components and led to smaller Tg difference of 36.7°C. For C1R20, Tg difference reached 46.8 °C which was still lower than that of the neat blend but it was larger than those of the blends containing C1R5 and C1R15.

Table 4 presents Tg of the blends containing the products of PC and PET reactive melt mixing under C2 condition. Tg difference of the blend containing C2R10, by 10°C lower than that of the neat blend, is 50°C. The addition of C2R20 decreased Tg difference of the neat blend to 53°C that was similar to C2R10.

The solubility versus mixing time was utilized to compare the amount (or the extension of reaction) and chemical structure of the samples. The solubility of C1R5 and C1R15 were in the decreasing section of the overall pattern in which the second one was lower (Fig. 2). This means that both of samples were comprised of copolymers with the same chemical structure with different contents. The structure included long block length copolymers and C1R15 had higher amount of copolymers than C1R5. This chemical structure of copolymers was in favor of PC/PET blend compatibilization that was shown by lower Tg differences of the blends containing C1R5 and C1R15 compared with that of non-compatibilized blend. The lower differences can be achieved by increasing the copolymer content. C1R20 was sampled in a mixing time which corresponded to the raising section of Fig. 1; indicating to the shorter block length of copolymers rather than those produced earlier (C1R15 and C1R5). This enabled C1R20 to compatibilize PC/PET blend, but with the achieved level of compatibility that was lower in comparison to those reached by C1R5 or C1R15. This was understood by a drop in ΔT_g of neat blend after mixing it with C1R20 but larger Tg difference than those attributed to C1R5 and C1R15.

The reactive melt mixing products prepared under C1 and C2 condition not only affected Tg of the blend components but also they influenced PET crystallization which was evaluated through endothermic melting peaks depicted in Fig. 3 and related data is presented by Tables 3 and 4.

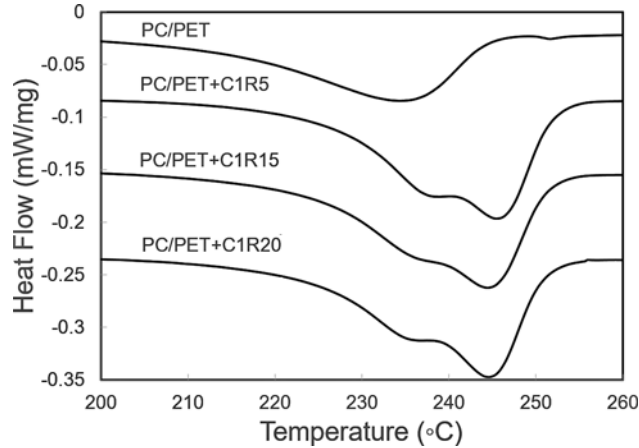


Figure 3. Endothermic melting peaks from DSC analysis of PC/PET blends with and without C1 series products.

PET in the pure blend had a melting point centered at 234°C. For prepared products with C1 condition, a shoulder appeared higher than 234°C. The temperature corresponding to the shoulder changed in the narrow range of 231 to 232°C for all C1 series but the main peak temperature appeared at 240, 243 and 242°C, for C1R5, C1R15 and C1R20 in the order given.

Inclusion of the products of C2 series into PC/PET blends formed a main endothermic melting peak with a shoulder at lower temperature (not shown here). While the melting temperature of PET component in PC/PET blend, which centered at 234°C, for the blends containing C2 series appeared at 244°C. The shoulder centered at 236°C for C2R10 and 235°C for C2R20.

PET crystallization in PC/PET blend was hindered by PC component which led to lower melting point in comparison to that of PET alone [27]. Mixing the blend with products of C1 series led a portion of PET molecules to crystallize, with a mean melting point slightly lower than that of PET in the neat blend, while the remaining PET molecules took part in crystallization with higher melting point. The copolymers within C1 series, as mentioned before, were responsible for compatibilization of PC/PET blends relating to the structure and content of copolymers. The blend compatibilization in which PC is made miscible with PET may result in the latter molecules to have lower melting points with respect to their neat blend. Kong et al. [28] studied crystallization of PC and PET reactive blending by Hoffman-Week model in which they attributed the reduction of PET equilibrium melting point (T_m°) to miscibility of PC in PET. Beside T_m° , a similar behavior including lower melting point of shoulder in comparison to that of PET in neat blend was expected and it was observed in this work. PET molecules, which were relieved of PC effects, formed the main endothermic melting peak at higher temperatures. Fig. 4 shows the upper melting temperature of PET versus T_g difference of PC/PET blends as an index of the acquired compatibility.

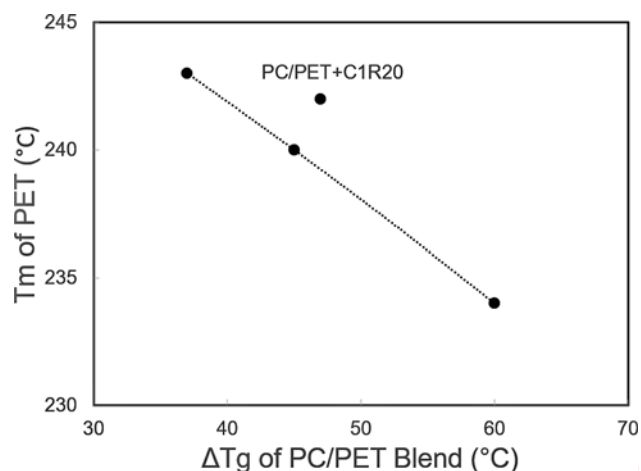


Figure 4. Melting temperature of second endothermic peak of PET versus T_g difference of PC and PET.

PET melting point of the blends was lowered by higher difference in T_g . The reduction of melting point was smaller for C1R5 with respect to C1R15 or C1R20 which were relatively the same. In other words, more compatibilization of the blends resulted in higher melting points although there was no difference between C1R15 and C1R20. With C1R20, a less blend compatibility was achieved but the melting temperature of PET component, based on its T_g difference, was higher than expected. This may be attributed to the different structure of the copolymer in C1R20 with shorter block length than those of C1R5 or C1R15. The share of higher melting temperature crystals from the whole PET endothermic melting peak is represented by their corresponding enthalpy ratio ($\Delta H_2/\Delta H$). As Figure 5 shows, the lower T_g difference has given higher enthalpy ratios.

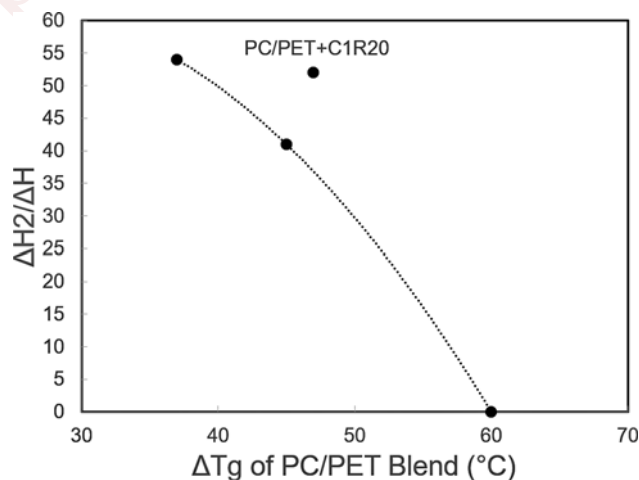


Figure 5. Enthalpy ratio of higher melting temperature peak to total PET enthalpy versus T_g difference of PC

and PET.

Mixing the blend with C1R15 instead of C1R5 decreased Tg difference of the blend which resulted in higher enthalpy ratio. For C1R20, this ratio was somehow lower than that of C1R15 but it was still higher than that of C1R5. Similar to the main melting peak temperature, the corresponding fraction of its crystals showed a good dependency on the amount and not on the type of PC and PET copolymers.

C1R15 corresponded to the dip in solubility diagram (figure 1) and among C1 product series led to the minimum Tg difference and the maximum melting point and enthalpy ratio of the second endothermic melting peak. In this sample the high content of copolymers with long block length is the responsible of these behaviors.

In opposite to C1 series products, here for C2 series there was an increase for shoulder melting points with respect to that of PET in the neat blend. This may be related to lower compatibilizing ability of C2 in comparison to C1 series which resulted in lower miscibility of PC in PET. Suppresses the impact on melting temperature and the higher melting point could be expected. The ratios of $\Delta H_2/\Delta H$ were the same for C2R10 and C2R20. Table 4 presents the melting temperatures and the relevant enthalpies.

The copolymers of C2 series had somehow the same structure and quantities. The identical ability of C2 series, based on relatively the same Tg differences, to compatibilize PC/PET blend resulted in the same effects on PET crystallinity. That has been shown by the same melting temperatures and enthalpy ratios of PET component after addition of C2 series products into the blend.

The presence of C1 and C2 series products in PC/PET blends affected thermal properties including Tg difference, Tm and crystallinity of PET phase depending on copolymer content and structures. Higher content and longer block length of copolymers, which comes from decreasing part of solubility pattern versus mixing time, decreased Tg difference and at the same time increased Tm and enthalpy ratio of the shoulder in the melting endothermic peak. On the other words, higher level of compatibility between PC and PET phases increases the portion of PET molecules could take part thicker crystals. In comparison of copolymer structure and its content, the effect of latter one is bigger.

Morphology

Figure 6 illustrates the SEM image of sample which is used for evaluating the compatibilization effects.

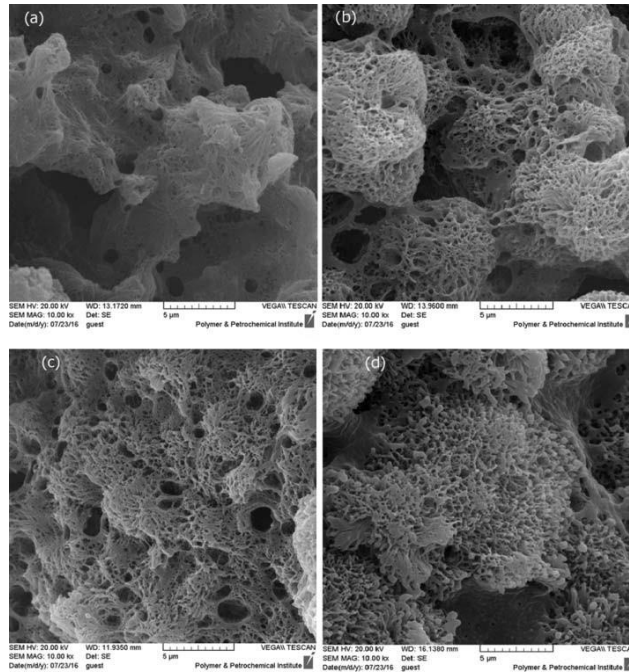


Figure 6. SEM micrographs of the etched cross-section of non-compatible PC/PET blend (a), compatibilized blend with C1R5 (b), compatibilized blend with C1R15 (c) and compatibilized blend with C1R20 (d).

SEM image reveals the morphology of PC/PET blends consisted of a matrix-droplet type with large size of dispersed phase (Fig. 6a). The addition of C1R5 to the blend made a sponge-like structure. In comparison with the uneven dispersion of PET droplets in the pure blend, in the presence of C1R5 a more uniform dispersion and smaller size PET particles were created in the PC matrix. But the large PET particles could be still found (Fig. 6b). PET dispersed phase morphology was unified with C1R15 addition (Fig. 6c). The large particles which could be found in the presence of C1R5 were eliminated by C1R15 addition. With employing C1R20, the morphology was unique and completely different (Fig. 6d). The morphology discrepancy may be related to the structural differences.

SEM results are in agreement with solubility and thermal properties through T_g difference and PET crystallinity ; indications of different compatibilizing effects on the products of C1 series. PC/PET blend with 70:30 composition shows two T_g corresponding to its components (figure 2 and table 3). SEM image of pure blend (figure 6a) comprises of coarse disperse-matrix morphology in agreement of thermal analysis results. Addition of C1R5 contains long block length copolymers of PC and PET made the blend partially miscible through smaller T_g difference and formation a shoulder in the melting endothermic peak of PET. In the SEM image, better dispersion of PET particles in PC matrix is clear (figure 6b). By C1R15, higher amount of

copolymers made the blend more compatible than that contained C1R5 because of smaller Tg difference and more pronounced shoulder of melting peak. As figure 6c shows a more uniform morphology of PET dispersed particles was appeared. C1R20 has copolymers with short block length copolymers and its morphology is somehow similar to C1R5 contained blend. In this case the achieved level of compatibility is lower than that of C1R15 contained blend.

We have developed a new strategy through the reactive melt blending to enhance the PC and PET miscibility with copolymer addition. The introduced technique helps to produce suitable compounds made of PC and PET copolymers for compatibilization of PC/PET blends at desired levels. The presented correlation between solubility and thermal properties made this strategy easy to achieve.

CONCLUSION

In this study attempted to enhance the PC/PET blend miscibility with copolymer and reactive melt blending. 5 wt% of compatibilizers in C1 and C2 condition were able to compatibilize 70:30 of PC/PET blend composition ratio. The decreased Tg difference of blend components and smaller PET particle size uniformly distributed in PC phase proved that the blend compatibilization has improved, because of the PC and PET presence in copolymer simultaneously. The change in solubility with mixing time was related to the amount and structure of copolymers. Tg difference of blend components was measured by DSC technique which showed a good correlation between them. For C1 series product, with the same copolymer structure, the higher copolymer content made lower difference in Tg. By changing the structure of copolymer including the shorter block length, Tg difference increased. For C2 series product, relatively the same amount of copolymers with identical structure resulted in similar Tg differences. PET crystallinity was affected by addition of C1 and C2 series through formation of the main endothermic melting peak at higher temperatures than that of PET in the neat blend, besides its shoulder formation. Crystallization in the shoulder region was affected by miscibility of PC and PET while the main endotherm showed crystallization under less negative effect of PC component. The melting temperature and enthalpy ratio of the main endotherm were mainly functions of copolymer content and not its structure. In actual fact, PET crystallization could not differentiate the reactive blending products during mixing time especially when copolymer structure changed.

ACKNOWLEDGMENTS

The authors wish to express their gratitude to the Research and Technology of National Petrochemical Company (NPC-R&T) for its financial support.

REFERENCES

1. Chirayil CJ, Joy J, Maria HJ, Krupa I, Thomas S (2016) Polyolefin Compounds and Materials. 1st ed., Springer, 265-283
2. Quigley JP, Herrington K, Baird DG (2014) Enhanced electrical properties of polycarbonate/carbon nanotube nanocomposites prepared by a supercritical carbon dioxide aided melt blending method. *Polym* 55: 6167-6175
3. Jazani OM, Arefazar A, Peymanfar MR, Saeb MR, Talaei A, Bahadori B (2013) The influence of NBR-g-GMA compatibilizer on the morphology and mechanical properties of poly (ethylene terephthalate)/polycarbonate/NBR ternary blends. *Polym- Plast Technl* 52: 1295-1302
4. Zarrintaj P, Moghaddam AS, Manouchehri S, Atoufi Z, Amiri A, Amirkhani MA, Nilfroushzadeh M A, Saeb M R, Hamblin M R, Mozafari M (2017) Can regenerative medicine and nanotechnology combine to heal wounds? The search for the ideal wound dressing. *Nanomedicine* 12: 2403-2422
5. Khonakdar HA, Jafari SH, Mirzadeh S, Kalae MR, Zare D, Saeb MR (2013) Rheology-morphology correlation in PET/PP blends: Influence of type of compatibilizer. *J Vinyl Addit Techn* 19: 25-30
6. Mohammadi Y, Khonakdar HA, Jafari SH, Saeb MR, Golriz M, Wagenknecht U, Heinrich G, Sosnowski S, Szymanski R (2015) Simulation of Microstructural Evolution During Reactive Blending of PET and PEN: Numerical Integration of Kinetic Differential Equations and Monte Carlo Method. *Macromol Theor Simul* 24: 152-167
7. Jazani O M, Rastin H, Formela K, Hejna A, Shahbazi M, Farkiani B, Saeb MR (2017) An investigation on the role of GMA grafting degree on the efficiency of PET/PP-g-GMA reactive blending: morphology and mechanical properties. *Polym Bull* 74: 4483-4497
8. Jazani OM, Arefazar A, Jafari SH, Saeb MR (2011) Study on the effect of processing conditions on the impact strength of PP/SEBS/PC ternary blends using Taguchi experimental analysis. *J Polym Eng* 31: 237-241

9. Pesetskii S, Jurkowski B, Filimonov O, Koval V, Golubovich V (2011) PET/PC blends: Effect of chain extender and impact strength modifier on their structure and properties. *J Appl Polym Sci* 119: 225-234
10. Ishigami A, Kodama Y, Wagatsuma T, Ito H (2017) Evaluation of Structures and Morphologies of Recycled PC/PET Blends Fabricated by High-Shear Kneading Processing. *Int Polym Proc* 32: 568-573
11. Meziane O, Guessoum M, Bensedira A, Haddaoui N (2017) Thermal characterization of reactive blending of 70PC/30PET mixtures prepared in the presence/absence of samarium acetylacetonate as a transesterification catalyst. *J Polym Eng* 37: 577-586
12. Fiorini M, Berti C, Ignatov V, Toselli M, Pilati F (1995) New catalysts for poly (ethylene terephthalate)/ bisphenol a polycarbonate reactive blending. *J Appl Polym Sci* 55: 1157-1163
13. Guessoum M, Haddaoui N (2006) Influence of the Addition of Tetrabutyl Orthotitanate on the Rheological, Mechanical, Thermal, and Morphological Properties of Polycarbonate/Poly (Ethylene terephthalate) Blends. *Int J Polym Mater* 55: 715-732
14. Mbarek S, Jaziri M, Carrot C (2006) Recycling poly (ethylene terephthalate) wastes: Properties of poly (ethylene terephthalate)/polycarbonate blends and the effect of a transesterification catalyst. *Polym Eng Sci* 46: 1378-1386
15. Pereira PS, Mendes LC, Abrigo RE (2008) Changes in properties of PET/PC blend by catalyst and time. *Int J Polym Mater* 57: 494-505
16. Godard P, Dekoninck J, Devlesaver V, Devaux J (1986) Molten bisphenol-A polycarbonate—poly (ethylene terephthalate) blends. II. Kinetics of the exchange reaction. *J Polym Sci Pol Chem* 24: 3315-3324
17. Mendes LC, Pereira PS (2013) Solid state polymerization: its action on thermal and rheological properties of PET/PC reactive blends. *Polímeros* 23: 298-304
18. Carrot C, Mbarek S, Jaziri M, Chalamet Y, Raveyre C, Prochazka F (2007) Immiscible blends of PC and PET, current knowledge and new results: rheological properties. *Macromol Mater Eng* 292: 693-706
19. Huang Z, Wang LH (1986) Infrared studies of transesterification in poly (ethylene terephthalate)/polycarbonate blends. *Macromol Rapid Comm* 7: 255-259
20. Swoboda B, Buonomo S, Leroy E, Cuesta JL (2007) Reaction to fire of recycled poly (ethylene terephthalate)/polycarbonate blends. *Polym Degrad Stabil* 92: 2247-2256
21. Carraro C, Tartari V, Pippa R, Pilati F, Berti C, Toselli M, Fiorini M (1996) Reactive blending of commercial PET and PC with freshly added catalysts. *Polym* 37: 5883-5887

22. Zhihui Y, Yajie Z, Xiaomin Z, Jinghua Y (1998) Effects of the compatibilizer PP-g-GMA on morphology and mechanical properties of PP/PC blends. *Polym* 39: 547-551
23. Jeziórska R (2001) PET/RPP/PC blends by two stage reactive extrusion: effect of polypropylene reactively functionalized with an oxazoline group on morphology and mechanical properties. *Macromol Symp Wiley Online Library*, 21-28
24. Ma H, Hao J (2011) Ordered patterns and structures via interfacial self-assembly: superlattices, honeycomb structures and coffee rings. *Chem Soc Rev* 40: 5457-5471
25. Xue ML, Yu YL, Sheng J, Chuah HH, Geng CH (2005) Compatibilization of poly (trimethylene terephthalate)/polycarbonate blends by epoxy. Part 1. Miscibility and morphology. *J Macromol Sci Phys* 44: 317-329
26. Xue ML, Yu YL, Sheng J, Chuah HH, Geng CH (2005) Compatibilization of poly (trimethylene terephthalate)/polycarbonate blends by epoxy. Part 2. Melting behavior and spherulite morphology. *J Macromol Sci Phys* 44: 331-343
27. Marchese P, Celli A, Fiorini M (2004) Relationships between the molecular architecture, crystallization capacity, and miscibility in poly (butylene terephthalate)/polycarbonate blends: A comparison with poly (ethylene terephthalate)/polycarbonate blends. *J Polym Sci Pol Phys* 42: 2821-2832
28. Kong Y, Hay J (2002) Miscibility and crystallisation behaviour of poly (ethylene terephthalate)/polycarbonate blends. *Polym* 43: 1805-1811

Captions of figures

Figure 1. Solubility versus mixing time for C1 and C2 processing condition with dichloromethane as the solvent.

Figure 2. Tg of PC and PET components for blends with and without C1 series products.

Figure 3. Endothermic melting peaks from DSC analysis of PC/PET blends with and without C1 series products.

Figure 4. Melting temperature of second endothermic peak of PET versus Tg difference of PC and PET.

Figure 5. Enthalpy ratio of higher melting temperature peak to total PET enthalpy versus Tg difference of PC and PET.

Figure 6. SEM micrographs of the etched cross-section of non-compatible PC/PET blend (a), compatibilized blend with C1R5 (b), compatibilized blend with C1R15 (c) and compatibilized blend with C1R20 (d).

Caption of Tables

Table 1. PC and PET Reactive blending conditions.

Table 2. Sampling times during PC and PET reactive melt blending under C1 & C2 mixing conditions.

Table 3. Thermal properties of PC/PET blend components after compatibilization by C1 series products.

Table 4. Thermal properties of PC/PET blend components after compatibilization by C2 series products.

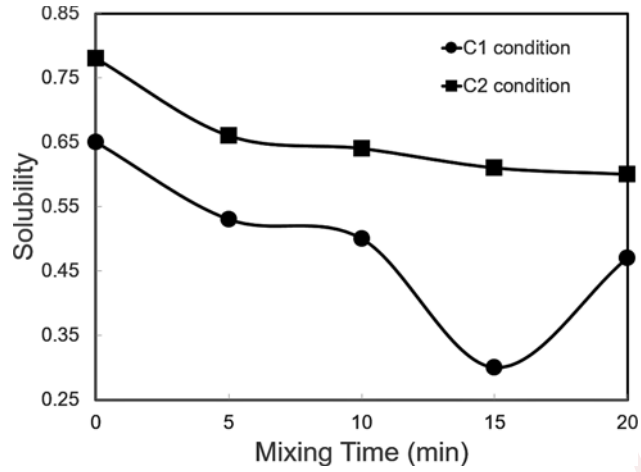


Figure 1. Solubility versus mixing time for C1 and C2 processing condition with dichloromethane as the solvent.

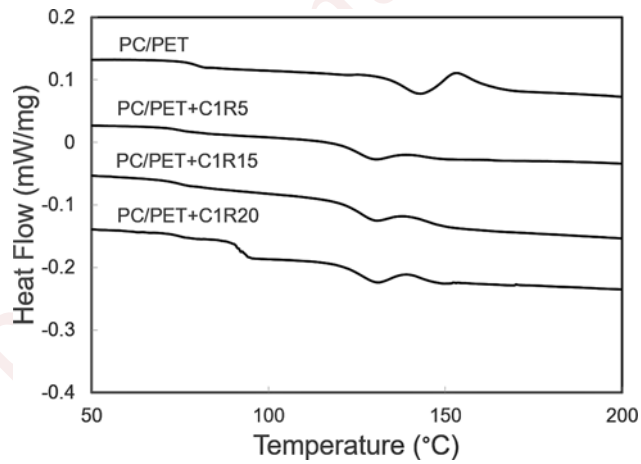


Figure 2. Tg of PC and PET components for blends with and without C1 series products.

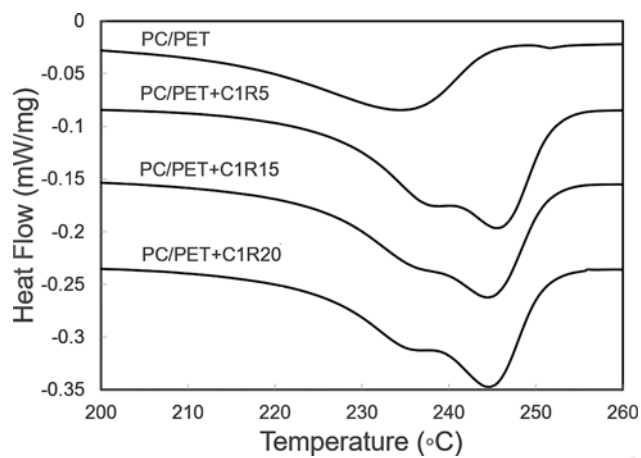


Figure 3. Endothermic melting peaks from DSC analysis of PC/PET blends with and without C1 series products.

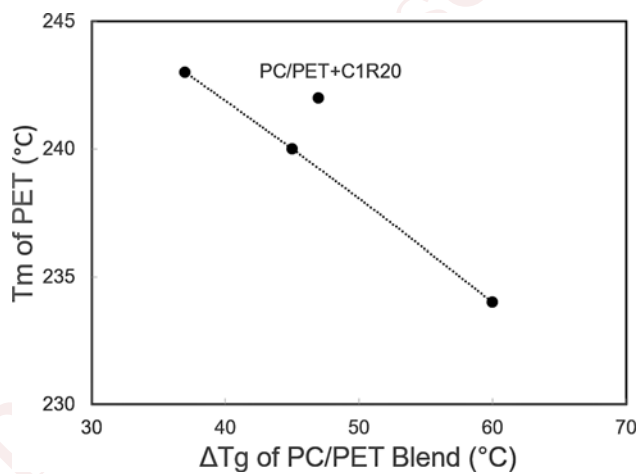


Figure 4. Melting temperature of second endothermic peak of PET versus Tg difference of PC and PET.

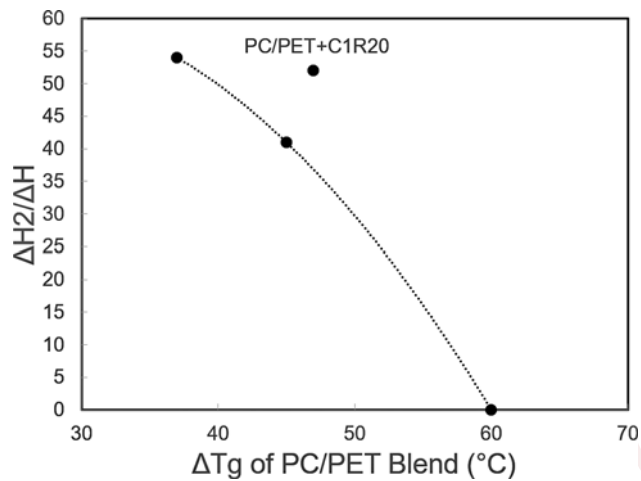


Figure 5. Enthalpy ratio of higher melting temperature peak to total PET enthalpy versus Tg difference of PC and PET.

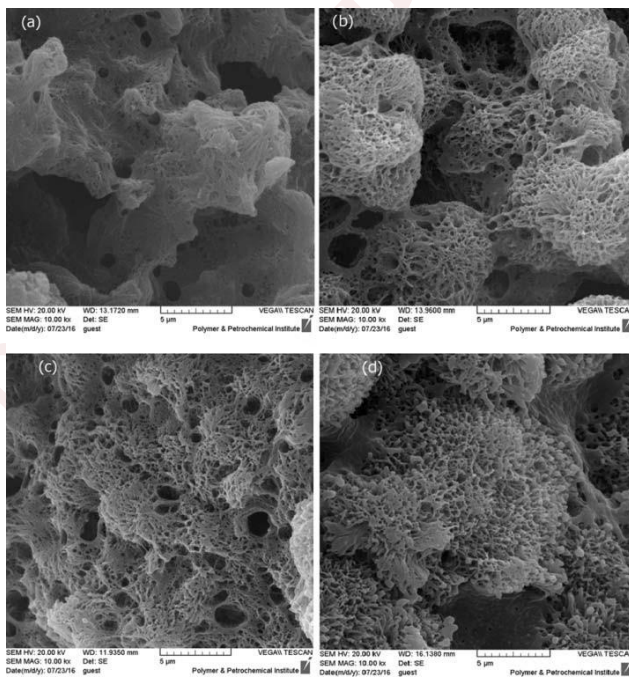


Figure 6. SEM micrographs of the etched cross-section of non-compatible PC/PET blend (a), compatible blend with C1R5 (b), compatible blend with C1R15 (c) and compatible blend with C1R20 (d).

Table 1. PC and PET Reactive blending conditions.

Sample code	T (°C)	Premixing time (min)	Rotor speed (rpm)	Catalyst content (wt %)
C1	280	15	50	0.20
C2	270	15	30	0.15

Table 2. Sampling times during PC and PET reactive melt blending under C1 & C2 mixing conditions.

Condition Code	Mixing time (min)			
	5	10	15	20
C1	C1R5		C1R15	C1R20
C2	-	C2R10	-	C2R20

Table 3. Thermal properties of PC/PET blend components after compatibilization by C1 series products.

Sample code	T _g ^{PET} (°C)	T _g ^{PC} (°C)	ΔT _g (°C)	T _{m1} (°C)	T _{m2} (°C)	ΔH ₁ (J/g)	ΔH ₂ (J/g)	ΔH ₂ /ΔH (%)
Neat PC/PET	78	138	60	234	-	8.12	-	0
PC/PET+C1R5	80	125	45	231	240	5.51	3.88	41
PC/PET+C1R15	82	119	37	232	243	4.48	5.19	54
PC/PET+C1R20	75	122	47	232	242	3.92	4.28	52

Table 4. Thermal properties of PC/PET blend components after compatibilization by C2 series products.

Sample code	T _g ^{PET} (°C)	T _g ^{PC} (°C)	ΔT _g (°C)	T _{m1} (°C)	T _{m2} (°C)	ΔH ₁ (J/g)	ΔH ₂ (J/g)	ΔH ₂ /ΔH (%)
Pure PC/PET	78	138	60	234	-	8.12	-	0
PC/PET+C2R10	71	122	50	236	244	5.79	5.56	49
PC/PET+C2R20	70	123	53	235	244	6.32	5.93	48